Numerical Simulation Of Small-Size Aggregate Accumulation Structure Under Dynamic Water Conditions

Weitao Liu[1,2], Chunhui Yang[1,2], Yanhui Du[2,3]

[1]*College of Energy and Mining Engineering, Shandong University of Science and Technology, Qingdao, Shandong 266590, China, skych521@163.com*

[2]*Shandong University of Science and Technology State Key Laboratory of Mine Disaster Prevention and Control, Qingdao, Shandong 266590, China*

[3]*College of Safety and Environmental Engineering, Shandong University of Science and Technology, Qingdao, Shandong 266590, China*

Abstract

The flow velocity is the key factor to determine the effect of dynamic water grouting. The accumulation body accumulated in the water passing roadway can effectively reduce the flow velocity. In this paper, non-spherical particles are used to simulate the accumulation of aggregates in roadways. The accumulation effect and force chain distribution of 5-10 mm small-sized aggregates in pipeline flow are calculated by the CFD-DEM method. Combined with IMAGE-J software, the anisotropic porosity and average porosity are obtained. The effect of dynamic water on the accumulation effect of small-sized aggregates and its influence on the accumulation porosity are analyzed.

Keywords: Dynamic water grouting, CFD-DEM, aggregate accumulation, numerical simulation, pore structure

Introduction

The movement of aggregate in dynamic water can be regarded as a kind of sediment movement under specific boundary conditions. When the aggregate is thrown into the water from the top of the dynamic water. The particles produce resistance to the fluid, and the fluid also produces drag force on the aggregate particles. The drag force is the force of the fluid on the relatively moving object, including pressure and shear force (viscous force). The size of the drag force is determined by a variety of physical quantities, which is the most important factor in the migration of aggregate particles and the basis for studying the influence of dynamic water on the morphology of aggregate deposits. In 1879, French scientists proposed the concept of drag force and the theory of bed load motion (Du Boys 1879). At the beginning of the century, Gilbert studied the movement of sediment through flume experiments (Gilbert 1914). Then Meyer-Peter used the empirical analysis method of isolated factors to establish the bed load transport rate formula based on the flume test data (Meyer-Peter *et al*. 1934). Sha summarized and put forward the basic law hypothesis of the critical velocity of sediment movement, and proved that the effective velocity of the open channel is the main factor to determine the amount of sand carried by flowing water (Sha 1996). Zhang and Dou adopted the principle of resistance superposition to derive a unified settling velocity formula for single-particle sediment in the stagnation zone, transition zone, and turbulent zone (Zhang 1998; Dou 1999).

Compared with irregular aggregate particles, the pore characteristics and permeability characteristics of regular shape particles such as circular particles are now more clear (Furnas 1928; Matuttis *et al*. 2000; Horsfield 1934; Stovall *et al*.1986; Isaia *et al*. 2003). As a kind of irregular granular material, the structure's internal pore structure composed of aggregate particles is relatively complex. The shape, gradation, and compactness of aggregate particles will affect the pore structure of the deposit, and then affect the permeability characteristics of the deposit (Peng *et al*.2020). It is difficult

to quantify the entire pore network. Studies have shown that pore characteristics at the particle scale are closely related to the stress characteristics and conductivity between particle materials. The emergence of discrete element numerical simulation technology provides a new technical means for people to study the system composed of a large number of granular particles. This method can accurately describe the velocity, position, force, and other parameters of a single particle in a particle group. The pore law of aggregate deposits can be obtained directly or indirectly through the above parameters. The CFD-DEM coupling calculation method calculates the interaction force between fluid and particles through momentum exchange, forming a mesoscopic simulation method for studying the coupling of particles and fluid. This paper uses the CFD-DEM coupling calculation method to study the structure of aggregate particle accumulation under dynamic water impact.

Numerical simulation parameter setting

Determination of roadway parameters

Mine roadway has strict design standards, most of the roadways arranged in the working face of coal mines are rectangular section roadways. When a water rush occurs in the working face, these roadways arranged in the working face often become the channel of water spreading to other working areas. This kind of roadway that plays a connected role in the water rush is called an "over-current roadway". For the CFD-DEM simulation method, before the numerical simulation, it is necessary to adjust the prototype roadway and study the similarity criteria. The roadway with a length and width of 4m and a rectangular section is selected as the prototype of simulation calculation.

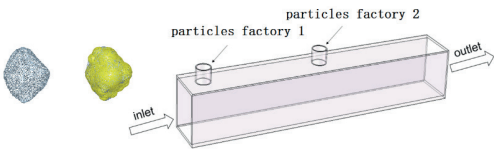

***Figure 1** Particle model and flow field model*

The Length similarity, Area similarity, and Volume similarity are

$$\frac{L'}{L} = \frac{l'}{l} = C_l \quad (1)$$

$$C_A = \frac{A'}{A} = \frac{l^2}{l^2} = C_l^2 \quad (2)$$

$$C_V = \frac{V'}{V} = \frac{l^3}{l^3} = C_l^3 \quad (3)$$

Where L is the characteristic length of the roadway, A is the section area, V is the section volume, the set length ratio Cl = 20, and the length and width of the model roadway are 20cm. Based on the geometric similarity, the kinematic similarity can be determined, such as speed similarity, time similarity, acceleration similarity, and flow similarity.

EDEM pellet property setting

In the engineering practice of dynamic water grouting and water interception, the particle size of aggregate is mostly between 5 and 50mm, and the large size aggregate is used as the "skeleton" of the structure and plays the role of water resistance. Particles with relatively small particle sizes are used to fill the gaps in the "skeleton" and act as an interception. 5-10mm small-size particles were selected as the research object for CFD-DEM coupling calculation.

To make the simulation calculation more realistic, the particle shape is fitted using the EDEM software MultiSphere option, as shown in Figure. 1. The aggregate particle calculation parameters are set up in Table 1.

Fluent flow field setting

The movement of water inrush flow in the roadway can be approximately regarded as pipeline flow, and the length, width, and height of the flow field model are set to 150cm, 20cm, and 20cm respectively. The initial flow velocity at the entrance is 0.3m/s. The distance between the two particles factory and the water inlet is 10cm and 75cm respectively. The overall flow field model is shown in Figure 1.

For practical engineering, in the process of aggregate transportation, part of the gravitational potential energy will be transformed into the kinetic energy of the aggregate particles. When the aggregate enters the water tunnel, there will be a certain

Table 1 Solution parameter setting for aggregate particles

Young modulus	Poisson ratio	Coefficient of restitution	Coefficient of sliding friction	Coefficient of rolling friction	Particle density
E(N/m^2)	v	a	f_1	f_2	ρ (kg/m^3)
5×10^6	0.3	0.4	0.4	0.1	2450

initial velocity. Because there are many factors affecting the initial velocity, it is difficult to be characterized by calculation. Therefore, an initial velocity of 0.4 m/s is given directly.

Numerical simulation results and analysis

Determination of accumulation angle and porosity of accumulation body in the pipeline under anhydrous condition

To determine the influence of dynamic water on aggregate accumulation, the accumulation angle and porosity of the particles are determined by EDEM software before the coupling calculation, and the accumulation pattern is shown in Figure. 2.

Slice analysis is performed on EDEM using its Slices function, slicing along the x-axis, and y-axis directions of the accumulation to obtain the cross-sectional structure of the accumulation at that location, as shown in Figure. 3. Use IMAGE J to binarize the section and measure it using a measuring tool, as shown in Figure. 3. Divide the area of the white area within the designated area by the total area of the area, and the result obtained can be approximately considered as the porosity of the accumulation in that section.

The data as shown in Table 2 are obtained after the area calculation of each section.

From it, we can see that the natural accumulation state of aggregate, the various section porosity is not much change, porosity fluctuates around 39.7%, the overall pore, particle distribution is relatively uniform, accumulation body y-axis section close to the isosceles triangle, accumulation Angle is 32, on both sides of the wall on the influence of aggregate accumulation is not obvious.

Changes of aggregate morphology and flow field during the aggregate accumulation

The ratio of surface area to mass of the same shape particles will be different. At the same density, the large size particles will sink faster in the water than the small size particles, and the impact of fast water velocity will make this situation more obvious. As shown in Figure. 4. A.

Set the water flow velocity at the inlet to 0.3m/s, The movement morphology of the particle group has undergone significant changes compared to Figure. 4. A. As shown in Figure. 4. B.

When the aggregate particles are initially accumulated, by the friction between the particles and the friction between the particles and the tube wall, the low-speed water flow is

Figure 2 *Particle accumulation morphology in the pipeline*

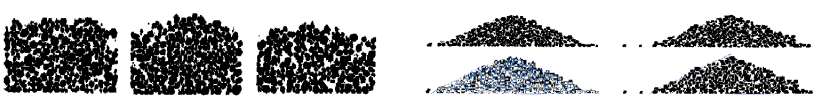

Figure 3 *Chart of the accumulation of body*

Table 2 Porosity of each section of the accumulation body

Number	x-axis 1	x-axis 2	x-axis 3	x-axis 4	x-axis 5	x-axis 1	x-axis 2
Porosity	39.62%	39.75%	39.65%	39.62%	40.12%	39.79%	39.86%

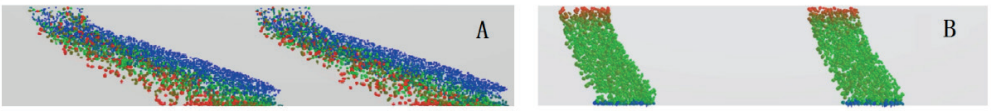

Figure 4 The movement morphology of the particle group

insufficient to cause the accumulated stable particles to move again, as shown in Figure. 5.

According to the setting, the generation speed and grading of the particle factories are the same. As the aggregates continue to accumulate, there is a significant difference in the accumulation shape of the adjacent two accumulation bodies. As shown in Figure. 5.

In the later period of aggregate accumulation, it is difficult for aggregate particles of 5-10mm particle size to raise the height of the whole accumulation body as shown in Figure. 5. Because the decrease of the Water cross-section makes the water flow velocity above the accumulation body increase, it is difficult to retain the small particle size particles on the top of the accumulation body. At this time, the velocity cloud atlas of the flow field is shown in the figure, and the flow velocity at the outlet is about 0.2 m/s, as shown in the Figure. 6, the water flow rate decreases significantly from the simulation.

From the above simulation results, it can be seen that the accumulation form of aggregates is not only related to the size, shape, and grading of aggregate particles but also to factors such as water flow velocity. Accurately predicting the shape of aggregate accumulation is difficult, but we can use numerical simulation calculations to determine whether particles of specific size, grading, and quantity can form an effective stacking structure at a specific speed.

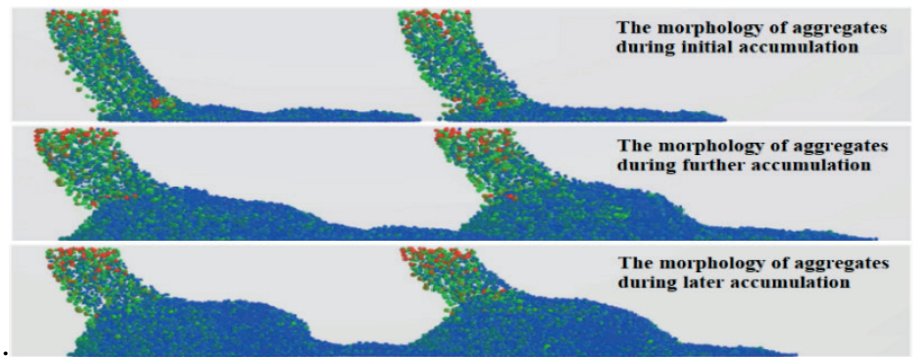

Figure 5 The morphology of aggregates accumulation

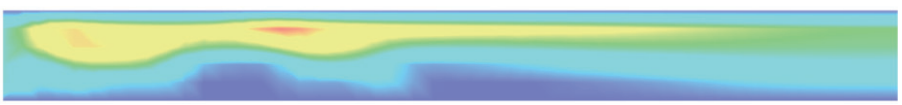

Figure 6 The velocity cloud atlas of the flow field in the later stage of aggregate accumulation

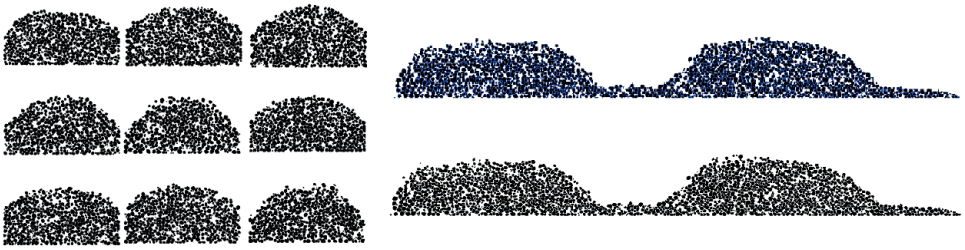

Figure 7 Accumulacking section under dynamic water impact

Treatment and analysis of the internal structure of accumulation body under dynamic water impact

The accumulated aggregate accumulation body was sectioned, binarized, measured, and counted by IMAGE J, as shown in Figure. 7.

The statistical results are shown in Table 3. From the statistical results we can conclude, the porosity of the upstream face section is relatively high, with the lowest porosity in the middle of the accumulation body away from the inflow direction; from the direction of water to the direction of water, the pores of the aggregate accumulation body decrease first and then rise. The bottom of the accumulation body is close to the center, and the porosity is the lowest. The dynamic water impact makes the aggregate accumulation porosity anisotropic, and the accumulation porosity along the y-axis is significantly higher than along the x-axis.

The simulation results were post-processed using Python to obtain a force chain distribution diagram of the accumulation body, as shown in Figure. 8. According to the calculated contact force, the force chain is divided into three levels for coloring. The contact force of red, green, and blue colors decreases sequentially, and the contact force can confirm the reliability of the structure from the side. The greater the contact force, the closer the bonding between particles. On the contrary, the smaller the contact force, the looser the particle bonding and the lower the strength. It is obvious that under this condition, the contact force distribution of the whole accumulation body is layered, and the blue force chain is the region where the accumulation body is the most vulnerable and most prone to structural instability.

Conclusion

Firstly, injecting aggregates into the water roadway can effectively reduce the flow

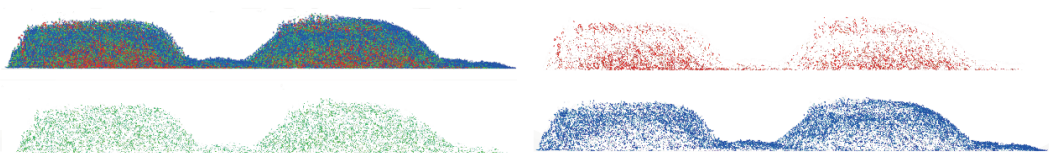

Figure 8 Force chain distribution diagram of accumulation body

Table 3 The porosity of each section of the accumulation body under dynamic water impact

Number	x-axis 1	x-axis 2	x-axis 3	x-axis 4	x-axis 5	x-axis 6
Porosity	37.50%	37.07%	36.50%	36.80%	37.68%	38.12%
Number	x-axis 7	x-axis 8	x-axis 9	x-axis 10	The y-axis section	
Porosity	37.90%	36.45%	36.48%	37.22%	38.78%	

velocity of the dynamic water. Under this simulated condition, the presence of an accumulation body reduces the flow velocity from 0.3m/s to 0.2m/s.

Secondly, the aggregate accumulation pattern of 5-10mm particle size is greatly affected by the dynamic water. When the accumulation body reaches a certain height, it is difficult to retain the smaller aggregate particles above the accumulation body. In the dynamic water state, the porosity of the accumulated aggregate will appear anisotropy, and the porosity distribution is not uniform and has certain regularity.

Finally, Due to the impact of dynamic water and the aggregate's gravity, the force chain distribution of the accumulation body is not uniform, and the particle structure near the surface layer of the accumulation body is loose, which is prone to structural instability so that the overall structure of the accumulation body is destroyed.

References

Du Boys P. Le (1879) Rhone et les rivieres a lit affouillable. [J] Annales des Ponts et Chaussees, Series 5,1879,18:141-195.

Gilbert G. K (1914) Transportation of debris by running water [J] Professional Paper U.S. Geological Survey,1914(86).

Meyer-Peter E, Muller R (1948) Formulas for bed-load Transport [C] Paper No.2, Proceedings of Second Meeting International Association for Hydraulic Research,1948:39-64.

Sha YQ. (1996) Introduction to Sediment Dynamics [M]. Beijing; China Industrial Press, 1996.

Zhang RJ. (1998) Dynamics of fluvial sedimentation [M]. Beijing; China Water Conservancy and Hydropower Press, 1998.

Dou GR. (1999) On the starting flow rate of sediment [J]. Sediment Research, 1999, (6): 1-9.

C. C. Furnas (1928) Bureau of Mines Reports of Investigation, No, 2894, 1928.

Matuttis HG, Luding S, Herrmann HJ. (2000) Discrete element simulations of dense packings and heaps made of spherical and non-spherical particles. Powder Technology, 109:278-292.

Horsfield HT. The strength of asphalt mixtures[J]. Journal of the Society for Chemical Industry, 1934, 53(2): 107–115.

Stovall T, De Larrard F, Buil M. (1986) Linear packing density model of grain mixtures [J]. Powder Technology, 1986, 48(1): 1–12.

Isaia GC, Gastaldini ALG, Moraes R. (2003) Physical and pozzolanic action of mineral additions on the mechanical strength of high-performance concrete[J]. Cement and Concrete Composites, 2003, 25(1): 69–76.

Peng JY, Zhang JF, Shen ZZ, *et al* (2020) Effect of grain shape on pore characteristics and permeability of coarse-grained soil [J]. Rock and Soil Mechanics, 2020, 41(02);592-600. DOI:10.16285/j.rsm.2019.0066.